# Characterization of gas-liquid interfacial microplasma used for metallic nanoparticles fabrication

V. Burakov[1], M. Chuchman[2], V.Kiris[1], M. Nedelko[1],
A. Shuaibov [2], N. Tarasenko[1]

[1]*B. I. Stepanov Institute of Physics, National Academy of Sciences of Belarus, Nezalezhnasti Ave. 68, 220072 Minsk, Belarus*
[2]*Uzhgorod national university, Pidgirna str. 46, 88000, Uzhgorod, Ukraine*

A gas-liquid interfacial microplasma generated between a capillary (needle) and liquid (distilled water) surface in ambient air without and with flowing argon as working gas was characterized by optical emission spectroscopy. The electron density of the microplasma generated in air was estimated to be 1-2×$10^{11}$ $cm^{-3}$ in the positive column and 2-9×$10^{12}$ $cm^{-3}$ in the cathode layer. Concentrations of NO and OH species measured from their emission intensities were about $10^{16}$ $cm^{-3}$. The vibrational temperature (0,15 - 0,33eV) determined based on the experimental emission from the $N_2$ second positive system increased with increasing discharge current and was more than twice higher than the gas temperature, which indicates the non-equilibrium state of the microplasma. Both temperatures were found to be dependent on the discharge parameters.

## 1. Introduction

In recent years, electrical discharge plasmas with liquid electrodes (plasma in contact with liquid) have attracted much attention for various technological applications, including synthesis of nanoparticles (NPs) [1]. In the discharge with liquid electrode, plasma is formed between an electrode in the gas phase and another immersed into the electrolyte solution. Igniting the microplasma results in the current flow through the electrolyte and reactions are observed at the anode and cathode. At the anode, oxidation reactions lead to dissolution of the solid metal into metal cations which are then reduced at the cathode by the microplasma to nucleate metal NPs. These observations suggest that gas-phase electrons can react with a solution at the plasma–liquid boundary to drive electrochemistry. Microplasma–liquid interactions have therefore initiated a new synthetic approach that is different from both standard liquid electrochemistry as well as from the submerged discharge method.

Recently, several groups used microplasmas generated between a hollow capillary cathode and liquid aqueous solution anode for nanomaterial synthesis [2-4].

However, physics of discharges between solid metal and liquid electrodes is not fully understood; there is no complete theoretical description of the discharges of this type. Only a few studies have been reported on the properties of this microplasma-liquid system. Nevertheless, parameters of nanoparticles synthesized by microplasma-assisted method depend on the plasma parameters such as the electron density, electron temperature, and gas temperature, which in turn, are largely dependent on the discharge current and the gas flow rate.

Information about the properties of a gas-discharge plasma transport processes and plasma parameters can be obtained on the basis of spectroscopic, electrical and spatial resolved investigation of the glow discharge. These data allow predicting the course of redox reactions and their influence on the synthesis of nanoparticles during processing of the solution by electric discharge plasma.

The results of the optical and electrical characterization of the microplasmas for different values of the discharge current and the gas flow are discussed in the present paper.

## 2. Experimental details

A schematic diagram of the experimental set-up is shown in Fig. 1. One metallic electrode made of Ag, Cu or Zn acting in the most experiments as anode was placed inside liquid. The discharge was ignited between a stainless-steel capillary electrode or copper needle electrode and the surface of liquid. Distilled water or the solution consisting of 1 mM $HNO_3$ with 10 mM glucose (fructose) or without these stabilizers were used as working liquids in our experiments. The acid was used to increase the solution conductivity; glucose and fructose are stabilizers that prevent uncontrolled particle growth and agglomeration. A stainless steel capillary tube (500 μm inside diameter, 5 cm length) or copper needle was located at a distance of 1-8 mm above the liquid surface and served as one of the electrodes. The second electrode (metal plate of copper, silver,

zinc) was submerged into liquid. The experiments were done with argon as the working gas flowing through the capillary tube and in air without argon gas flow. The argon flow rate was measured with a mass flow controller and can be varied from 10 to 45 sccm (cubic centimeters in standard conditions). The discharge was ignited by applying a high voltage using a dc power supply. The plasma was ignited when the voltage is increased to about 2 kV. A ballast resistor (0.1 - 0.4 MΩ) limits the current and provides stability to the discharge. The discharge current should be kept constant in the range of 1 - 5 mA in the regime with argon flow during the nanofabrication process and in the range 10 – 40 mA in the regime with air as working gas. So, two discharge regimes were studied: a low current glow discharge in argon flow (regime I) and high current atmospheric pressure glow discharge with air as a working gas (regime II)

Images of plasma were obtained with a digital camera. The selection of the radiation was carried out from the whole plasma area or from the discrete discharge zones located at 2, 4, 6 and 8 mm above the liquid surface.

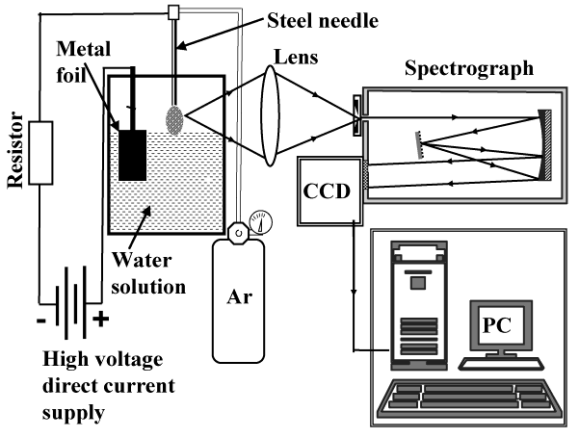


Fig. 1: Schematic diagram of the experimental set-up.

Spectroscopic studies of plasma were performed using a diffraction spectrograph equipped with a CCD linear array. The light emitted by the plasma was focused by lens with focal length 15 cm on the entrance slit of a spectrometer with a 1200 grooves/mm grating in order to investigate the spectral region from 280 nm to 700 nm. The operation of the detection system was controlled from a computer via a USB interface, using the software CCD Tool. The identification procedure took into account the spectral positions of the lines and their intensities (height of the line minus the background) in comparison to the relative intensities (or transition probabilities) indicated by the national institute of standards and technology (NIST) database.

## 3. Results and Discussion

The typical *I-V* curves of the microplasma for the different polarity of the liquid electrode are presented in Fig. 2.

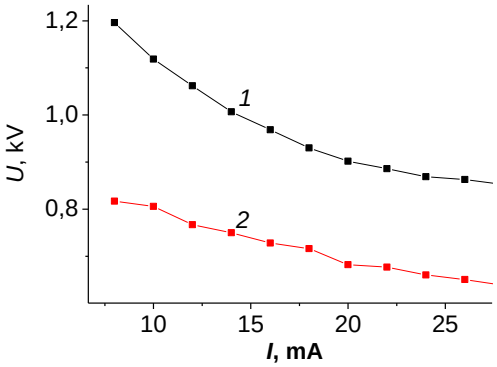


Fig. 2. Current-voltage curves for the discharge with distilled water cathode (*1*) and anode (*2*).

The electron density $n_e$ was estimated from electrical parameters of the discharge: $n_e = j/(E\mu_e e)$, where $j$ is the current density, $E$ is the electric field, $\mu_e$ is the electron mobility, and $e$ is the elementary charge. The electron density vs. current is shown in Fig. 3.

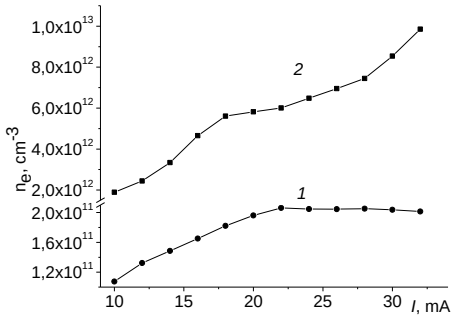


Fig.3. Dependence of the electron density in the positive column (1) and in the cathode sheath (2) on the discharge current

For calculations of plasma parameters we used normal conditions, which allow estimating of the maximal values of the electron concentration related to the near threshold regimes and breakdown. Thus, for the cathode region the maximal value of the electric field $E = 1.7 \times 10^8$ V/m, the size of the cathode layer of $2.6 \times 10^{-6}$ m and the electron mobility of 0.0134 $m^2/s$ were obtained. For positive column these values were E = 7.7 kV/m, the electron mobility of 0.6398 $m^2/s$.

The values of the electron density in the positive column and in the cathode layer were estimated to be 1-2×$10^{11}$ $cm^{-3}$ and to 2-9×$10^{12}$ $cm^{-3}$, respectively. The concentrations of chemically active molecules and radicals estimated from the NO and OH emission intensities were about $10^{16}$ $cm^{-3}$.

A typical emission spectrum of the discharge in air between copper needle and water cathode is shown in Fig. 4. As can be seen from the Fig. 4 the spectrum is dominated by radiation of $N_2$ 337.1 nm (transition $C^3\Pi_u$ - $B^3\Pi_g$ (0; 0) ) and OH 306,4 nm (transition ($A^2\Sigma^+$ - $X^2\Pi_i$ (0; 0)). We could also observe with less intensities the presence of molecular NO generated bands below 273 nm, the second positive system of $N_2$ (280–450 nm) and emission of hydrogen $H_\alpha$ 656.3 nm line.

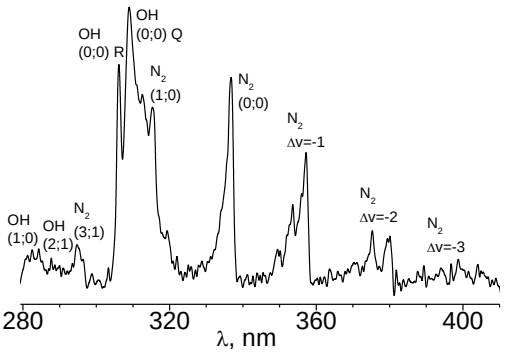


Fig.4. Typical emission spectrum of the glow discharge with liquid-based distilled water electrode at a current of 17 mA.

Most likely, the OH bands are due to the vapor phase at the plasma-water interface while the nitrogen bands are probably caused by interaction of the plasma with the surrounding air.

It was found that the H and OH emission intensities grew rapidly with current increasing, while emission of nitrogen molecules decreased sharply with current increasing up to 19 mA and then was not practically changed. The analysis of the emission spectra from different spatial zones along the plasma pinch showed that the hydroxyl emission intensity increased with current increasing from 12 to 32 mA in the whole discharge area. The re-distribution of the emission intensity of $N_2$ and NO with a current growth was observed in the cathode region where improved formation of nitrogen oxides occured. In general, the spatial intensity distribution points to enhancing of oxidation efficiency in the near cathode region saturated with water vapor and changing geometry with increasing a discharge current.

Based on the experimental emission from the $N_2$ second positive system the vibrational temperature was determined (0,15 - 0,33eV) by plotting the populations distribution of the vibrational states. The vibrational temperature increased with increasing discharge current and was more than twice higher than the gas temperature, which indicates the non-equilibrium state of the discharge microplasma.

Emission spectra of the gas–liquid interfacial discharge plasma generated in argon flow in the process of Ag nanoparticles synthesis were recorded for different argon flow rates. The main components of the spectra were found to be Ag lines and $N_2$ bands which disappeared when the argon flow rate was increased from 15 to 60 sccm (Fig.5).

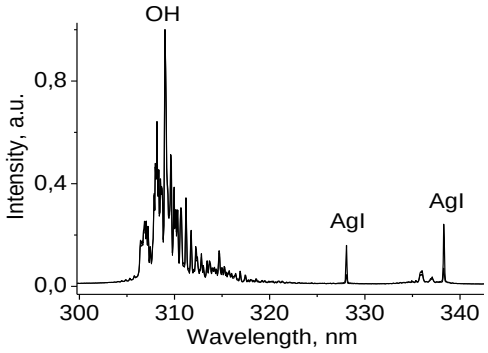


Fig.5. Emission spectrum of the gas–liquid interfacial discharge plasma generated in argon under 60 sccm rate of the argon flow.

Plasma temperature was evaluated using relative intensity values of silver lines Ag I λ=3280.7 and 3382.9 nm. According to the evaluation data the plasma temperature decreases from 4000 to 2000 K with the increase of the argon flow rate.

A computer code was developed to evaluate emission spectra of the discharge depending on its parameters and experimental conditions. The code allows calculating spectral radiation intensity of the plasma volume along the observation line, where space-time distributions of the plasma parameters are defined. These data are preset in a parametrical way using *a priori* knowledge on space-time evolution of the plasma volume reflecting the discharge behavior. The radiation transfer equation was solved in a *line-by-line* approximation, i.e. a number of the points used for a chosen spectral line is quite enough to account for its profile.

Typical absorption spectra of the colloidal solutions prepared by the gas–liquid interfacial discharge with a silver anode and a TEM photograph of the prepared silver NPs are shown in Fig 6, 7. For silver nanoparticles the spectrum exhibited the characteristic plasmon absorption band with a peak located at 400 nm. This band characteristic for

spherical Ag nanoparticles appeared and grew in intensity with increasing discharge burning time.

TEM analysis of the as-grown NPs confirms that the particles are slightly agglomerated, quasi spherical with a mean size of about 15-20 nm.

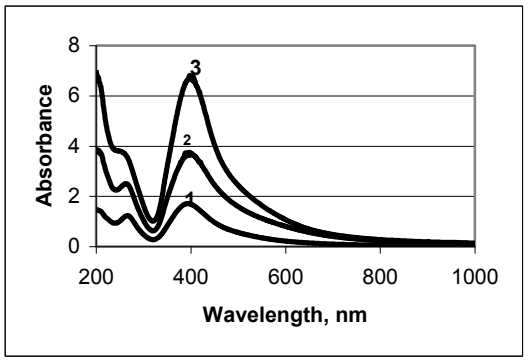


Fig.6. Absorption spectra of Ag nanoparticles prepared by the gas–liquid interfacial discharge. Curves *1, 2, 3* correspond to the discharge burning time of 1, 2 and 3 min, respectively.

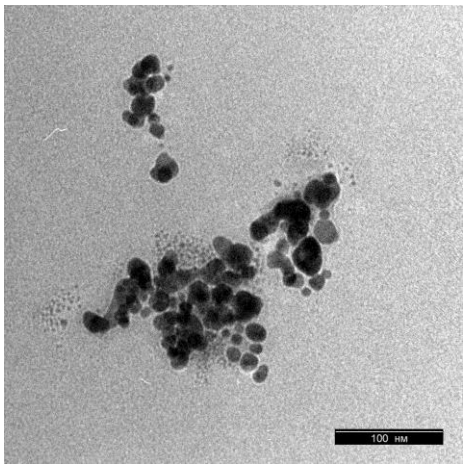


Fig.7. TEM image of Ag nanoparticles prepared by the gas–liquid interfacial discharge in 0,01M fructose solution. The scale bar is 100 nm.

Further experiments are necessary to fully understand the mechanism for particle nucleation and growth. We consider that the particle size is controlled by the reaction volume, which can be defined as a small region near the microplasma-liquid interface. Our experimental observations suggest that the particle nucleation is driven by the electromigration of metallic cations to this region and subsequent electrochemical reduction by the microplasma. A growth then occurs until the particles are carried out of the reaction volume by convective or diffusive flow back into the bulk solution. Thus, it can be inferred that the size distribution of the as-grown particles is practically unaffected by the process time.

**Conclusion**

A microplasma generated under atmospheric pressure between a metallic capillary and liquid has been characterized. Two discharge regimes: a low current glow discharge in argon flow and a high current atmospheric pressure glow discharge with air as a working gas were studied. The measured current-voltage characteristics suggest that the discharges are in glow-like modes. The electron density of the microplasma generated in air was estimated to be $1\text{-}2\times10^{11}$ $cm^{-3}$ in the positive column and $2\text{-}9\times10^{12}$ $cm^{-3}$ in the cathode layer. Concentrations of NO and OH species measured from their emission intensities were about $10^{16}$ $cm^{-3}$. The vibrational temperature (0.15 - 0.33eV) determined based on the experimental emission from the $N_2$ second positive system increased with increasing discharge current and was more than twice higher than the gas temperature. The difference between the vibrational and rotational temperatures indicates the non-equilibrium state of the microplasmas. Both temperatures were found to be dependent on the discharge parameters.

The developed discharge configurations have shown to be compact, simply-to-use with a good stability and can be used for effective radicals' production, water purification and nanoparticles fabrication.

**Acknowledgements**

This work is partially financed by the Belarusian Foundation for Fundamental Researches under grant No.F 13K-086 and Ukrainian Foundation for Fundamental Researches under grant No. F 54.1/030. We also acknowledge the support from European Community, COST Action TD1208.

**References**

[1] D. Mariotti, R.M. Sankaran, *J. Phys. D: Appl. Phys.* **43**, (2010) 323001.

[2] J. Patel, L. Nemcova, P. Maguire, W.G. Graham and D Mariotti, *Nanotechnology*, **24** (2013) 245604.

[3] N.Shirai, S.Uchida and F.Tochikubo, *Jap. J. of Appl. Phys.*, **53** (2014) 046202.

[4] V.Burakov et al *Plasma Physics and Technology* **1**, (2014), 127.